Acta Radiologica
2014, Vol. 55(7) 855–863

DOI: 10.1177/0284185113506900
acr.sagepub.com

Time-dependent diffusion tensor changes of optic nerve in patients with indirect traumatic optic neuropathy

J Li[1], W Shi[3], M Li[2], Z Wang[1], H He[2], J Xian[1], B Lv[2] and F Yan[1]

Abstract

Background: Indirect traumatic optic neuropathy (ITON) is a devastating cause of permanent visual loss. Axonal degeneration, the characteristic pathological change of ITON, cannot be assessed by conventional imaging. Diffusion tensor imaging (DTI) has been widely used as a sensitive non-invasive imaging technique to obtain information on axonal integrity.
Purpose: To study time-dependent changes in ITON patients with DTI and to provide imaging evidence for clinical diagnosis and therapy.
Material and Methods: We enrolled 28 subjects with unilateral ITON who underwent detailed ocular examinations and magnetic resonance imaging (MRI) examinations. The differences between injured optic nerve (ON) and contralateral ON were tested. The patients were divided into three groups based on time (from injury to examination). Groups 1, 2, and 3 corresponded to the time taken from injury to examination: $<$7 days, 7–30 days, and $>$30 days, respectively. DT magnetic resonance imaging (MRI) differences among the groups were compared, including the relationship between diffusion parameters and mean thicknesses of the peripapillary retinal nerve fiber layer (RNFL) and ganglion cell complex (GCC) in the macular area.
Results: Compared with contralateral ON, we observed reduced fractional anisotropy (FA) of injured nerves in group 2. Reduced FA and decreased axial diffusivity ($\lambda//$) and increased radial diffusivity ($\lambda\perp$) and mean diffusivity (MD) of injured nerves were observed in group 3. The mean FA value of injured nerves showed a progressive decreasing trend, and mean $\lambda\perp$ value exhibited a progressive increasing trend. For injured eyes, the MD and $\lambda\perp$ increases strongly correlated with the decreased mean thicknesses of RNFL and GCC. Conversely, FA was significantly associated with mean RNFL thickness.
Conclusion: DT-MRI parameters could be useful biomarkers in detecting ON changes in ITON patients.

Keywords
Trauma, optic neuropathy (ITON), MRI, diffusion tensor imaging (DTI)

Date received: 16 June 2012; accepted: 1 September 2013

Introduction

Traumatic optic neuropathy is a devastating cause of permanent visual loss following contusive injuries to the head, particularly to the forehead (1), and indirect traumatic optic neuropathy (ITON) is the most common form (2,3). ITON is defined as traumatic loss of vision that occurs without external or initial ophthalmoscopic evidence of injury to the eye or its nerve (4). Although the degree of visual loss after indirect traumatic optic neuropathy can be quite variable,

[1]Department of Radiology, Beijing Tongren Hospital, Capital Medical University, Beijing, PR China
[2]Key Laboratory of Complex Systems and Intelligence Science, Institute of Automation, Chinese Academy of Sciences, PR China
[3]Department of Ophthalmology, Beijing Tongren Hospital, Capital Medical University, Beijing, PR China

Corresponding author:
Z Wang, Department of Radiology, Beijing Tongren Hospital, Capital Medical University, Beijing, PR China.
Email: cjr.wzhch@vip.163.com

approximately 50% of patients maintain "light perception" or "no light perception" vision (5).

No treatment, megadose corticosteroids, optic canal decompression surgery, or a combination of these are the present management options for ITON, but the optimal treatment remains controversial mainly because the lack of histologic data in the clinical examination (3,6,7). Short TI inversion recovery (STIR) magnetic resonance imaging (MRI) sequences can detect the high signal of swelling ON in early ITON, but this change is somewhat subjective and can be mild at the time of trauma or within the first few days afterwards. Apparent ON atrophy and ON sheath dilation would be detected more than 2 months post trauma (8), so conventional imaging cannot sensitively assess ITON. Furthermore, conventional imaging fails to accurately identify the underlying pathology. Therefore, the development of a non-invasive imaging technique to detect early changes and to evaluate ON axonal degeneration is important. Diffusion tensor imaging (DTI) is a sensitive technology for investigating central nervous system (CNS) white matter (WM) diseases and injuries (9–11). DTI utilizes anisotropic diffusion displacement-probability ellipsoids that are characterized by three eigenvalues ($\lambda1$, $\lambda2$, and $\lambda3$) and three eigenvectors. The average of the three eigenvalues is referred to as mean diffusivity (MD), $MD = (\lambda1 + \lambda2 + \lambda3)/3$. In CNS WM, the largest eigenvalue $\lambda1$ represents water diffusivity parallel to axonal fibers. It is referred to as $\lambda//$, or axial diffusivity. The water diffusivities perpendicular to the axonal fibers, $\lambda2$ and $\lambda3$, are averaged and referred to as $\lambda\perp = (\lambda2 + \lambda3)/2$, or radial diffusivity. Fractional anis-otropy (FA) was defined by the following equation:

$$FA = \sqrt{\frac{3}{2}\frac{(\lambda_1 - \bar{\lambda})^2 + (\lambda_2 - \bar{\lambda})^2 + (\lambda_3 - \bar{\lambda})^2}{\lambda_1^2 + \lambda_2^2 + \lambda_3^2}}$$

Given that the axonal structural integrity reflects the random displacement of water molecules (i.e. anisotropic diffusion), it is feasible to utilize DTI as a means to obtain information about axonal state (12). Mac Donald et al. (13), in a mouse model, showed that DTI was highly sensitive to experimental pericontusional white matter injury throughout the full range of assessed time points, and DTI signal changes could determine the approximate time since injury. ITON is a closed injury produced by force imparted to the skull and transmitted into the ON, and this could cause ON damage and subsequent axonal degeneration (2); therefore, we hypothesized that ITON could be investigated with DTI.

The aims of our study were to observe time-dependent ON changes in ITON patients with DT-MRI, which could reflect the axonal state and myelin degradation, and to investigate the relationships among DT-MRI parameters and the mean thicknesses of peripapillary retinal nerve fiber layer (RNFL) and ganglion cell complex (GCC) in macular areas.

Material and Methods

Subjects

The present study was conducted at the Beijing Tongren Hospital, Capital Medical University, China. Twenty-eight subjects (26 men, 2 women; mean age, 27.64 ± 10.51 years; range, 14–44 years) with unilateral ITON were enrolled. The contralateral eye served as a control to minimize variability among patients. Vehicle accidents (including bicycle and motorbike) were the main causes of trauma (53.57%). The majority of patients had poor visual acuity (VA) (from no light perception [NLP] to hand movement [HM], 71.43%) at first examination. The mean baseline intraocular pressure (IOP) of the injured eye was 15.07 ± 3.25 mmHg (Table 1). The time (from injury to examination) of two patients was >1 year. The time range (from injury to examination) of the other 26 patients was 2–95 days, median 15 days. At 1 or 3 months after the first examination, 13 patients went to review and underwent the second examination. So, we obtained 41 data groups of 28 patients totally.

Table 1. Demographic and clinical characteristics of unilateral ITON patients.

Characteristic	Total ($n = 28$)	
Age (years)	27.78 ± 10.51 (range, 14–44)	
Sex		
Male	26	92.85%
Female	2	7.15%
Eye		
Right	14	50.00%
Left	14	50.00%
Injury causes		
Vehicle/bicycle accident	15	53.57%
Assault	6	21.53%
Fall	7	25.00%
Baseline visual acuity		
NLP, LP, HM	20	71.43%
<20/200 to CF	3	10.71%
<20/40 to ≥20/200	2	7.15%
≥20/40	3	10.71%
Baseline IOP (mmHg)	15.07 ± 3.25(10–25.6)	

HM, hand movement; LP, light perception; NLP, no light perception.

Based on the time (from injury to first or second examination), the patients were divided into three subgroups. Groups 1, 2, and 3 included patients with time (from injury to examination) <7 days, 7–30 days, and >30 days, respectively. The time (from injury to examination) of four patients at two time points was >1 month for both. To avoid the bias arising from repetition, we only included data from one visit because we hypothesized that longer time would result in more evident DTI changes. Therefore, the earlier visit data were adopted to avoid overestimation of the results. At last, 37 patient data groups were included in the analysis and there were 10, 10, and 17 patients in Groups 1, 2, and 3, respectively. The corrected vision of the contralateral eye was more than 20/20 in each patient.

Each patient underwent high-resolution orbital computed tomography (CT) with a 64-slice multidetector CT (Philips Brilliance CT, Philips Medical Systems, Best, The Netherlands) to rule out the presence of optic canal fractures or bone fragments in the orbital apex. The patients underwent detailed ocular examinations, including visual acuity, slit-lamp biomicroscopy, Goldmann applanation tonometry, and fundus examination. Spectral domain optical coherence tomography (SD-OCT) examination was performed with the RTVue (Optovue Inc., Fremont, CA, USA). RTVue was used to generate images of ocular microstructures and employed a scanning laser diode with a wavelength of 840 ± 10 nm, which can perform 26,000 A scans/s with a depth resolution of 5 μm. In our study, the mean thicknesses of RNFL and GCC in the macular areas of all patients were performed on the same day as the MRI examination. RTVue OCT images were obtained by blinded examiners. Only good quality images, as defined by a signal strength index of ≥30 were used for the analysis.

MRI

All patients underwent MRI examination using a 1.5-Tesla magnet (GE Healthcare, Waukesha, WI, USA) scanner with an 8-channel head coil. Subjects were asked to close their eyes to minimize any effects of deliberate eye movement during the acquisition. Head motion was minimized by restraining foam pads.

Each subject was scanned using a high-resolution T2-weighted (T2W) fluid-attenuated inversion recovery sequences (FLAIR) sequence (TR, 9000 ms; TE, 120 ms; TI, 2125 ms; slices, 32; slice thickness, 4 mm; slice gap, 0.8 mm; field of view [FOV], $240 \times 210\,mm^2$; matrix size, 256×222) to detect any brain abnormalities, and any patient with abnormalities was excluded.

Axial T2W images of ON (TR, 3800 ms; TE, 102 ms; slices, 12; slice thickness, 3.5 mm; slice gap, 0.3 mm; FOV, $180 \times 180\,mm^2$; matrix size, 288×224) was obtained as the location sequence for the DTI.

Coronal ON DTI images were obtained using spin-echo echo-planar-imaging sequences with parallel acquisition. Coronal-oblique slices were set orthogonal to the nerves. The imaging coverage was from the optic papilla to the orbital apex of the ON (Fig. 1).

We used the following acquisition parameters for ON DTI: one b0 and six non-collinear gradient directions with $b = 600\,s/mm^2$; slices, 8; thickness, 5 mm; gap, 0; FOV, $22 \times 22\,cm^2$; acquisition matrix size, 128×128; NEX, 16; voxel size, $0.86 \times 0.86 \times 5\,mm^3$. The signal to noise ratio (SNR) was set at 35–40 in our study. The eddy current distortions and motion artifacts in the DT-MRI data were corrected using FMRIBs diffusion toolbox (FSL, Oxford, UK, http://www.fmrib.ox.ac.uk/fsl/fdt/index.html) (14,15).

The MD, FA, and eigenvalues (λ1, λ2, and λ3) of ON were calculated voxel-by-voxel using DTI Studio (Version 3.0, MRI Studio Software, Johns Hopkins University, Baltimore, MD, USA). All diffusion-weighted (DW) images were visually inspected for apparent artifacts due to head motion, and no significant image deterioration was found. Subsequently, the eddy current was eliminated by realigning all DW and non-DW images. The regions of interest (ROIs) were defined manually on the DW image consisting of two square 2×2 voxels. The ROIs were placed in the center of the nerve (Fig. 2) (16–18). The six elements of the diffusion tensor were calculated for each pixel using multivariate linear fitting. After tensor diagonalization, three eigenvalues and eigenvectors were obtained, and FA maps were calculated. The eigenvector associated with the largest eigenvalue was used as an indicator for fiber orientation. The color FA map images were also calculated from DW images. The intraorbital fourth layer of the nerve (about 2.0 cm behind the optic papilla) was used for the following analysis (19).

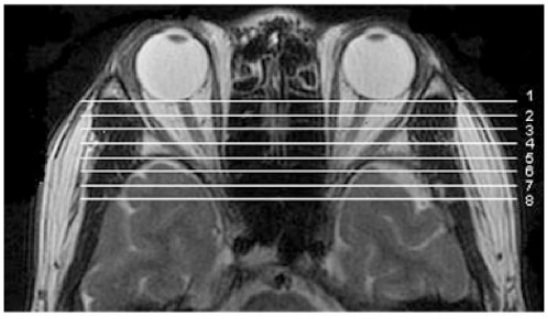

Fig. 1. Position of optic nerve slices on an axial view. There are eight slices from the anterior part (adjacent to the optic papilla) to the posterior part (near the orbital apex).

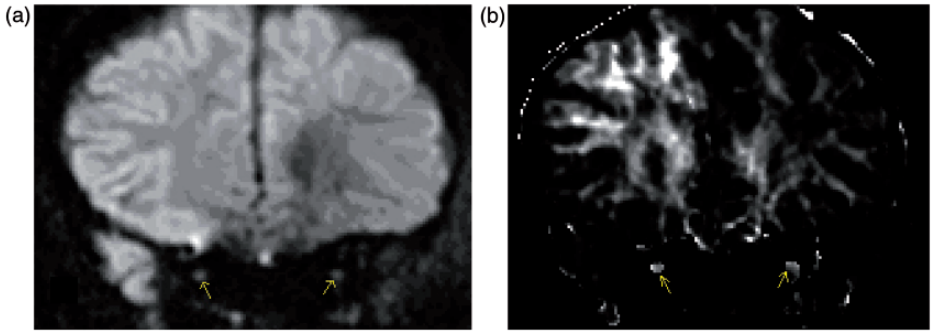

Fig. 2. ROI selection in the fourth slice of the optic nerve. (a) Diffusion-weighted image. (b) Fractional anisotropy map. The yellow arrow indicates the optic nerve.

Table 2. Diffusion parameters of injured nerves and contralateral nerves by ITON group.

Group	Parameter	Injured nerve	Contralateral nerve	*t*-value	*P* value
Group 1 ($n=10$)	FA	0.51 ± 0.10	0.54 ± 0.06	1.08	0.307
	MD	1.42 ± 0.21	1.53 ± 0.24	1.14	0.285
	$\lambda_{\|}$	2.32 ± 0.39	2.56 ± 0.29	1.72	0.120
	$\lambda_{\perp}$	0.97 ± 0.17	1.02 ± 0.23	0.55	0.598
	FA	0.40 ± 0.11	0.53 ± 0.06	3.96	0.002
Group 2 ($n=10$)	MD	1.68 ± 0.23	1.57 ± 0.19	1.18	0.271
	$\lambda_{\|}$	2.50 ± 0.30	2.61 ± 0.25	1.08	0.312
	$\lambda_{\perp}$	1.26 ± 0.33	1.06 ± 0.18	1.89	0.051
	FA	0.35 ± 0.08	0.53 ± 0.08	6.26	0.000
Group 3 ($n=17$)	MD	1.68 ± 0.20	1.55 ± 0.21	2.27	0.037
	$\lambda_{\|}$	2.34 ± 0.27	2.56 ± 0.24	3.74	0.010
	$\lambda\perp$	1.34 ± 0.20	1.04 ± 0.23	3.79	0.002

Axial, radial, and mean diffusivities ($\lambda_{\|}$, $\lambda\perp$, MD) are given in μm/ms. Fractional anisotropy is without units. All values are mean ± sd. ITON=Indirect traumatic optic neuropathy.
Group 1, the time (from injury to examination) was <7 days. Group 2, the time (from injury to examination) was 7–30 days. Group 3, the time (from injury to examination) was >30 days.

We certify that our research adhered to the tenets of the Declaration of Helsinki. All institutional and governmental regulations concerning the ethical use of human subjects were followed during this study, and informed consent was obtained from each subject.

Statistical analysis

Statistical analysis was performed using SPSS v13.0 (SPSS Inc., Chicago, IL, USA). Differences between injured ON and contralateral ON were explored using paired t-tests. One-way analysis of variance (ANOVA) test was used to compare the DT-MRI parameters among three subgroups at different time points. The DT-MRI parameters of two examinations of the same one patient were compared using paired t-tests. The relationships among the diffusion parameters of ON and mean thicknesses of peripapillary RNFL and GCC in the macular area were investigated using Pearson correlation analysis. Values of $P < 0.05$ were considered statistically significant.

Results

Diffusion parameters

In Group 1, no significant differences within ROIs were detected in DT-MRI measurements between injured and contralateral ONs. In Group 2, the mean FA ($t=3.96$, $P=0.002$) of injured ON was significantly reduced, and slightly increased $\lambda\perp$ of injured ON was found relative to contralateral ON, but the latter did not reach statistical significance ($t=1.89$, $P=0.051$; Table 2). In Group 3, significantly decreased FA ($t=6.26$, $P=0.000$; Table 2) and $\lambda//$ ($t=3.74$, $P=0.010$; Table 2) values and increased MD ($t=2.27$, $P=0.037$; Table 2) and $\lambda\perp$($t=3.79$,

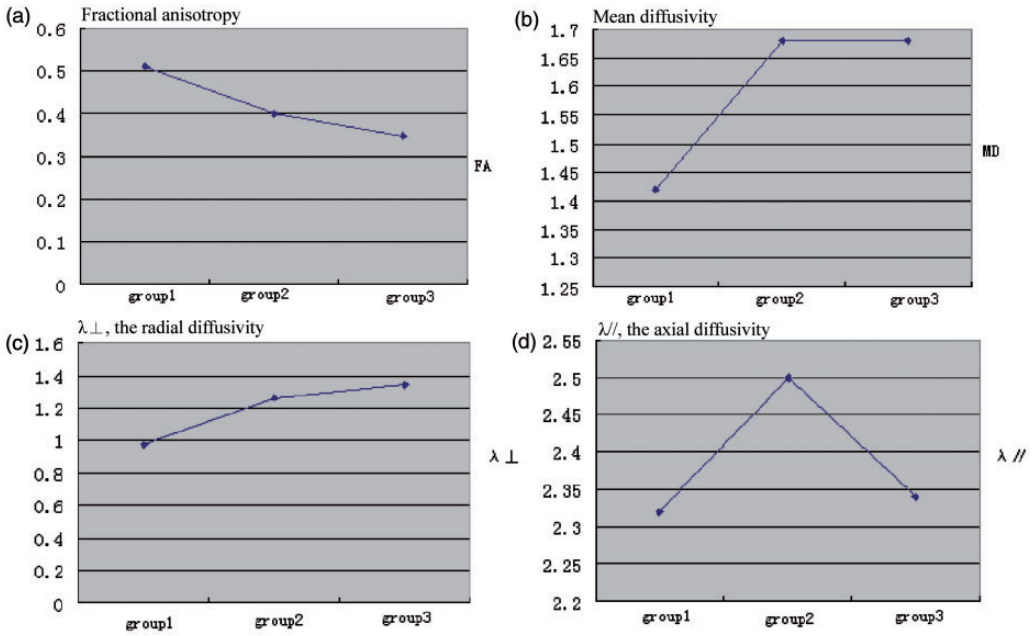

Fig. 3. Dynamic diffusion parameters changes in injured optic nerve. FA showed a progressive decreasing trend. MD was normal within 7 days after injury and elevated thereafter. λ⊥ showed a progressive increase trend. λ// decreased the first week following injury and then elevated from 7 days to 1 month after surgery before decreasing again at more than 1 month after injury.

Table 3. One-way ANOVA analysis of diffusion parameters of patients with ITON by group.

Parameter	Group 1 ($n=10$)	Group 2 ($n=10$)	Group 3 ($n=17$)	F value	*P* value
FA	0.51 ± 0.10	$0.40 \pm 0.11^*$	$0.35 \pm 0.08^*$	8.99	0.001
MD	1.42 ± 0.21	$1.68 \pm 0.23^*$	$1.68 \pm 0.20^*$	5.55	0.008
$\lambda_{\|\|}$	2.32 ± 0.39	2.50 ± 0.30	2.34 ± 0.22	1.00	0.379
λ⊥	0.97 ± 0.17	$1.26 \pm 0.33^*$	$1.34 \pm 0.20^*$	8.53	0.001

Axial, radial, and mean diffusivities ($\lambda_{\|}$, λ⊥, MD) are given in μm/ms. Fractional anisotropy is without units. All values are mean ± sd.
*$P < 0.05$ in Dunnett's t multiple comparisons when compared with first group.
ITON, indirect traumatic optic neuropathy.

$P=0.002$; Table 2) values were detected when injured and contralateral ONs were compared.

When DT-MRI parameters of three subgroups with different time points were compared, mean FA showed a progressive decreasing trend ($F=8.99$, $P=0.001$; Fig. 3, Table 3). Compared with Group 1, the mean MD values of Groups 2 and 3 both increased ($F=5.55$, $P=0.008$; Fig. 3, Table 3). The mean value of λ⊥ showed a progressive increasing trend ($F=8.53$, $P=0.001$; Fig. 3, Table 3). The injured ON showed an initial decrease in mean λ// in the first week after injury compared with the contralateral ON ($t=1.72$, $P=0.120$; Table 2). The mean λ// value in injured ON showed a trend towards increasing in Group 2 and decreased again in Group 3 ($F=1.00$, $P=0.379$; Fig. 3, Table 3).

We also found that mean FA decreased ($t=4.69$, $P=0.001$; Table 4) and mean λ⊥ increased ($t=3.03$, $P=0.010$; Table 4) over time when the DT-MRI parameters were compared between two examinations of the same patient.

Mean RNFL and GCC thicknesses

In Group 1, the mean thicknesses of RNFL and GCC were not significantly different between injured and contralateral eyes. In Groups 2 and 3, the average RNFL and GCC thicknesses in injured eyes were significantly smaller than those in controls (Group 2, RNF, $t=4.05$, $P=0.001$, GCC, $t=2.87$, $P=0.012$; Group 3, RNF, $t=14.56$, $P=0.000$, GCC, $t=9.77$, $P=0.000$; Table 5).

Correlation between diffusion parameters and RNFL and GCC thicknesses

Mean GCC thickness was significantly associated with mean RNFL thickness ($r = 0.619$, $P = 0.001$; Table 6). Increases in MD and $\lambda\perp$ were strongly correlated with decreases in the mean thicknesses of RNFL and GCC (MD with RNFL and GCC thickness, $r = -0.549$, $P = 0.001$, and $r = -0.625$, $P = 0.000$, respectively; $\lambda\perp$ with RNFL and GCC, $r = -0.630$, $P = 0.001$, and $r = -0.559$, $P = 0.002$, respectively; Table 6). FA was significantly associated with mean RNFL thickness ($r = 0.582$, $P = 0.001$; Table 6).

Discussion

A previous study demonstrated that force applied to the frontal bone could transfer to the intracanalicular segment of the ON (2). Because ON vasculature in the canal is pial, compression and contusion of the nerve produces a compartment syndrome whereby swelling exacerbates ischemia. The ON also suffers shearing injury under the fixed edge of the falciform dural fold just before it enters the optic canal (3). A histopathological study of 174 patients who died after closed head injury demonstrated evidence of hemorrhage in the ON sheath (83%), in the nerve interstitium (36%), and shearing lesions and ischemic necrosis of the intracanalicular and intracranial segments of the ON (20).

Diffuse axonal injury (DAI) is a consequence of sustained acceleration and deceleration forces that can shear axons and produce microscopic changes in the brain similar to ITON. Like ITON, DAI cannot be assessed by conventional imaging. However, DTI has been used to investigate diffuse DAI, and a direct comparison between DTI-detected WM integrity changes and histologic findings in an animal model of axonal injury suggested that DTI may be a valuable imaging tool for detecting diffuse axonal injury (10,21). Therefore, we used DTI to investigate ITON patients.

Challenges associated with DT-MRI of the ON are the small diameter of the nerve, artifacts caused by eye movement, and the susceptibility effects caused by nearby sinuses. In light of these, and despite using different sequences and protocols, it is remarkable that several different groups have reported similar values in healthy controls (MD $1.0–1.3 \times 10^{-3}$mm^2 s^{-1} and FA 0.4–0.6) (16–18,22). In our study, the mean FA and MD values of 28 control eyes were 0.54 ± 0.06 and $1.54 \pm 0.20 \times 10^{-3}$mm^2 s^{-1}, respectively. No paper was retrieved about using DTI to investigate ITON, so

Table 4. DT-MR parameters comparison between two time points ($n = 13$).

Parameter	First	Second	*t* value	*P* value
FA	0.44 ± 0.11	0.32 ± 0.10	4.69	0.001
MD	1.53 ± 0.19	1.69 ± 0.18	1.99	0.069
λ//	2.38 ± 0.18	2.29 ± 0.26	1.07	0.304
$\lambda_\perp$	1.11 ± 0.29	1.39 ± 0.21	3.03	0.010

Axial, radial, and mean diffusivities ($\lambda_\parallel$, $\lambda\perp$, MD) are given in μm/ms. Fractional anisotropy is without units. All values are mean ± sd.

Table 6. Correlation matrix of diffusion parameters, RNFL, and GCC.

Parameter	RNFL	GCC
FA	0.582(0.001)	0.331(0.091)
MD	–0.549(0.003)	–0.625(0.000)
$\lambda_\parallel$	–0.088(0.662)	–0.388(0.046)
$\Lambda_\perp$	–0.630(0.000)	–0.559(0.002)
RNFL	1.000	0.619(0.001)

GCC, ganglion cell complex; RNFL, retinal nerve fiber layer.

Table 5. Mean RNFL and GCC thickness of injured eyes and contralateral eyes at different time stage in ITON.

Group	Parameter	Injured eye	Contralateral eye	*t* value	*P* value
Group 1 ($n = 9$)	RNFL	112.97 ± 11.76	111.63 ± 15.00	0.34	0.742
	GCC	94.85 ± 9.42	96.66 ± 10.37	–1.11	0.301
Group 2 ($n = 10$)	RNFL	87.22 ± 11.94	104.44 ± 8.70	–4.05	0.001
	GCC	68.05 ± 26.04	92.17 ± 10.32	–2.87	0.012
Group 3 ($n = 8$)	RNFL	70.65 ± 3.18	101.96 ± 6.96	–14.56	0.000
	GCC	69.23 ± 5.97	95.04 ± 7.38	–9.77	0.000

GCC, ganglion cell complex; Group 1, the time (from injury to examination) was < 7 days; Group 2, the time (from injury to examination) was 7–30 days; Group 3, the time (from injury to examination) was >30 days; ITON, indirect traumatic optic neuropathy; RNFL, retinal nerve fiber layer.

we consulted many papers about DAI to explain our results.

When axonal injury occurs, centrifugal disintegration of the axonal cytoskeleton leads to sudden and rapid axon fragmentation. This stage is short-lived, lasting from several hours to days. At the same time, myelin sheaths that surround the axons become less tightly wrapped and eventually break apart and form ovoids. In the weeks following the precipitating injury, the microglia are activated and digests the axonal and myelin debris (12). Song et al. in a mouse model of retinal ischemia (23), performed serial diffusion ON measurements and showed that $\lambda//$ and $\lambda\perp$ could differentiate axonal from myelin damage during the course of degeneration. According to this animal study, $\lambda//$ showed a significant decrease in the first few days of degeneration, which corresponded to the disintegration of the axonal microstructure, whereas myelin remained intact. Five days after the initial injury, $\lambda\perp$ increased, which corresponded to myelin sheath degradation.

In Group 1, we observed that the mean $\lambda//$ of injured ON was reduced compared with the contralateral ON. In Group 2, the mean FA of injured ON was reduced, and $\lambda\perp$ increased relative to contralateral ON. Meanwhile, $\lambda//$ of the injured ON was slightly increased when compared with Group 1 (Table 2). Histological and electron microscopy results from a mouse traumatic brain axonal injury model (13) indicated that there were three distinct temporal phases of injury in pericontusional WM. According to this animal study, the predominant pathology in the first 24 h was relatively pure axonal injury without gliosis or demyelination, and the diffusion measurements changes were that $\lambda//\downarrow$,$\lambda\perp\approx$, FA$\downarrow$, and MD$\approx/\downarrow$. In the later acute stage (4 days), axonal injury was still marked, but gliosis became more pronounced. They hypothesized that DTI in the first 4 days would show a decreased axial diffusivity attributable to extensive axonal injury. This would, in turn, cause a marked reduction in relative anisotropy and a modest reduction in MD. In the subacute stage (7 days to 1 month), axonal injury became less apparent, and myelin thinning and active demyelination by macrophages was prevalent, while gliosis remained prominent. At the subacute stage, there would be an increase in radial diffusivity attributable to demyelination and reductions in axial diffusivity as a result of persistent axonal injury ($\lambda//\approx$, $\lambda\perp\uparrow$, FA$\downarrow$, and MD$\uparrow$) (13). Our research yielded similar results. We attributed the mean $\lambda//$ reduction in Group1 (the first 7 days after injury) to axonal injury without gliosis or demyelination. This difference did not reach statistical significance, which may be due to the small sample size. In Group 2, it appears that the second stage, i.e. 7 days to 1 month after injury, was the subacute stage of ITON. The main pathologic change during this stage was demyelination.

In Group 3 (injured over 1 month), we observed significantly decreased FA and $\lambda//$ values and increased MD and $\lambda\perp$ values compared with contralateral ON (Table 2). Similarly, a rat spinal cord injury model showed that $\lambda//$ in and surrounding a chronic spinal cord injury decreased at 12 weeks after injury. These changes may be maximal at the sites of greatest axonal loss, which would explain the correlation between decreasing $\lambda//$ values and decreasing numbers of labeled axons (24). Reduction in FA at this stage is due to a reduction in parallel diffusivity and an increase in perpendicular diffusivity. Increased MD was due to a marked increase in perpendicular diffusivity, while, decreased $\lambda//$ implied axonal loss. Therefore, we suggested that ITON began to enter the chronic stage after 1 month.

Although the loss of axons may be expected to increase water diffusion as it does in chronic cerebral infarcts (25,26), the $\lambda//$ in traumatically injured spinal cord and brain is not elevated; rather, it is less than that observed in normal tissue (24,27). Vorisek et al. (28) provided a possible explanation when they noted that there were both astrocyte proliferation and increased chondroitin sulfate proteoglycan expression in the extracellular matrix after experimental DAI, both of which may contribute to consistently decreased water diffusion.

We found that the mean macular thickness of GCC, which is the sum of the thicknesses of the retinal nerve fiber, ganglion cell, and inner plexiform layers (29) was significantly associated with mean RNFL thickness in injured eyes. A study on glaucoma suggested a correlation between the mean GCC and RNFL thicknesses in the intact hemisphere and thought that GCC thickness could be considered to represent damage of ganglion cells and their axons (30).

Our findings demonstrate that the degree of progressive axonal dieback in injured ON (mean thicknesses of GCC and RNFL) strongly correlated with the degree of abnormality in measured DTI parameters (MD, FA, and $\lambda\perp$). In a rat spinal cord injury model with greater axonal loss closer to the injury site, $\lambda\perp$ increased and $\lambda//$ decreased, which correlated with the greatest loss of axons (31). Therefore, it appeared that DTI parameters could reflect changes in axonal numbers.

We found that the mean FA value of injured nerves showed a progressive decreasing trend, and mean $\lambda\perp$ values showed a progressive increasing trend as the time since injury increased. When following the same patient over time, mean FA decreased and mean $\lambda\perp$ increased. The average thicknesses of RNFL and GCC of injured eyes were significantly thinner than those in contralateral eyes in the second and third stages.

These results suggest that neuronal and axonal degeneration are difficult to reverse in these stages.

There are some limitations to this study. Histologic validation was not possible, so our discussion of histological changes is speculative. In addition, the standard MRI of patients was not complete, so we could not provide more information about nerve diameters or areas. DT-MRI sequencing of the ON needs to be improved. However, the novelty of this study is the time-dependent DTI change observed in ONs of ITON patients without other traumatic findings, which, to our knowledge, has never been done before.

In conclusion, we observed time-dependent changes of DTI parameters could reflect the progression of axonal degeneration in ITON. We suggest that ITON patients with normal conventional imaging results could benefit from this objective non-invasive test because improved assessment techniques may facilitate the development of effective therapeutic strategies, aid in the clinical management of patients, and allow more accurate prognostic statements to be made at earlier times following injury.

Acknowledgements

We would like to thank all the patients who participated in this study.

Funding

This work was supported by the Beijing Keji Xinxing project (2004B36).

References

1. Awan AH. Case report. Traumatic optic neuropathy. Pak J Ophthalmol 2007;23:100–102.
2. Sadeghi-Tari A, Lashay AR, Tabassi A, et al. Visual outcome of traumatic optic neuropathy in patients treated with intravenous megadose of steroids. Acta Medica Iranica 2005;43:110–114.
3. Sarkies N. Traumatic optic neuropathy. Eye 2004;18:1122–1125.
4. Kovacić M, Gracner T, Gracner B. Indirect traumatic optic neuropathy–two case report. Coll Antropol 2001;25 (Suppl.):57–61.
5. Carta A, Ferrigno L, Salvo M, et al. Visual prognosis after indirect traumatic optic neuropathy. J Neurol Neurosurg Psychiatry 2003;74:246–248.
6. Yang WG, Chen CT, Tsay PK, et al. Outcome for traumatic optic neuropathy-surgical versus nonsurgical treatment. Ann Plastic Surg 2004;52:36–42.
7. Lee KF, Nor NIM, Yaakub A, et al. Traumatic optic neuropathy: a review of 24 patients. Int J Ophthalmol 2010;3:175–178.
8. Mavrakanas NA, Schutz JS. Feigned visual loss misdiagnosed as occult traumatic optic neuropathy: diagnostic guidelines and medical-legal issues. Surv Ophthalmol 2009;54:412–416.
9. Budde MD, Kim JH, Liang HF, et al. Toward accurate diagnosis of white matter pathology using diffusion tensor. Magn Reson Med 2007;57:688–695.
10. Mac Donald CL, Dikranian K, Song SK, et al. Detection of traumatic axonal injury with diffusion tensor imaging in a mouse model of traumatic brain injury. Expl Neurol 2007;205:116–131.
11. Sidaros A, Engberg AW, Sidaros K, et al. Diffusion tensor imaging during recovery from severe traumatic brain injury and relation to clinical outcome: a longitudinal study. Brain 2008;131:559–572.
12. Concha L, Donald WG, Matt Wheatley B, et al. Diffusion tensor imaging of time-dependent axonal and myelin degradation after corpus callosotomy in epilepsy patients. NeuroImage 2006;32:1090–1099.
13. Mac Donald CL, Dikranian K, Bayly P, et al. Diffusion tensor imaging reliably detects experimental traumatic axonal injury and indicates approximate time of injury. J Neurosci 2007;44:11869–11876.
14. Behrens T, Woolrich M, Jenkinson M, et al. Characterization and propagation of uncertainty in diffusion-weighted MR imaging. Magn Reson Med 2003;50:1077–1088.
15. Behrens TE, Johansen BH, Woolrich M, et al. Noninvasive mapping of connections between human thalamus and cortex using diffusion imaging. Nat Neurosci 2003;6:750–757.
16. Trip SA, Wheeler-Kingshott C, Jones SJ, et al. Optic nerve diffusion tensor imaging in optic neuritis. NeuroImage 2006;30:498–505.
17. Wheeler-Kingshott CA, Trip SA, Symms MR, et al. In vivo diffusion tensor imaging of the human optic nerve: pilot study in normal controls. Magn Reson Med 2006;56:446–451.
18. Kolbe S, Chapman C, Nguyen T, et al. Optic nerve diffusion changes and atrophy jointly predict visual dysfunction after optic neuritis. NeuroImage 2009;45:679–686.
19. Li M, Li J, He H, et al. Directional diffusivity changes in the optic nerve and optic radiation in optic neuritis. Br J Radiol 2011;84:304–314.
20. Crompton MR. Visual lesions in closed head injury. Brain 1970;93:785–792.
21. Wang JY, Bakhadirov K, Devous Sr MD, et al. Diffusion tensor tractography of traumatic diffuse axonal injury. Arch Neurol 2008;65:619–626.
22. Naismith RT, Xu J, Tutlam NT, et al. Disability in optic neuritis correlates with diffusion tensor-derived directional diffusivities. Neurology 2009;72:589–594.
23. Song SK, Sun SW, Ju WK, et al. Diffusion tensor imaging detects and differentiates axon and myelin degeneration in mouse optic nerve after retinal ischemia. NeuroImage 2003;20:1714–1722.
24. Arfanakis K, Haughton VM, Carew JD, et al. Diffusion tensor MR imaging in diffuse axonal injury. Am J Neuroradiol 2002;23:794–802.
25. Sotak CH. The role of diffusion tensor imaging in the evaluation of ischemic brain injury: a review. NMR Biomed 2002;15:561–569.
26. Takahashi M, Fritz-Zieroth B, Chikugo T, et al. Differentiation of chronic lesions after stroke in

stroke-prone spontaneously hypertensive rats using diffusion weighted MRI. Magn Reson Med 1993;30:485–488.
27. Schwartz ED, Shumsky JS, Wehrli S, et al. Ex vivo MR determined apparent diffusion coefficients correlate with motor recovery mediated by intraspinal transplants of fibroblasts genetically modified to express BDNF. Exp Neurol 2003;182:49–63.
28. Vorisek I, Hajek M, Tintera J, et al. Water ADC, extracellular space volume, and tortuosity in the rat cortex after traumatic injury. Magn Reson Med 2002;48:994–1003.
29. Takagi ST, Yoshiyuki K, Takeyama A, et al. Macular retinal ganglion cell complex thickness and its relationship to the optic nerve head topography in glaucomatous eyes with hemifield defects. J Ophthalmol 2011;2011:1–5.
30. Greenfield DS, Bagga H, Knighton RW. Macular thickness changes in glaucomatous optic neuropathy detected using optical coherence tomography. Arch Ophthalmol 2003;121:41–46.
31. Schwartz ED, Chin CL, Shumsky JS, et al. Apparent diffusion coefficients in spinal cord transplants and surrounding white matter correlate with degree of axonal dieback after injury in rats. Am J Neuroradiol 2005;26:7–18.